Response to the reviews of "Current status of ocean observation, ensemble reanalysis and CMIP6 models in describing Antarctic Bottom Water" by S. Chen, Liu, J., and X. Han

Response to comments by Reviewer #1

We would like to thank the reviewer for the helpful comments on the paper.

Major Comments

1. *The proposed subtype framework needs a clearer demonstration of robustness.*

The whole paper is built on the subdivision of AABW into WPBW, RSBW, and ALBW using a neutral density threshold and fixed salinity ranges. Since all later comparisons depend on this framework, I think the manuscript needs at least a basic sensitivity analysis showing whether the main subtype patterns remain stable under modest changes in the thresholds. At present, the classification is introduced and then used throughout the paper, but its robustness is not really demonstrated.

Response:

Thanks for the reviewer's constructive comments. We agree that it is important to demonstrate the physical robustness of the Antarctic Bottom Water (AABW) subtype classification framework used in this study. Therefore, we conducted a sensitivity analysis, which will be added to Section 2.3 (Sensitivity analysis) in the revised manuscript.

First, we only used the neutral density ($\gamma_n \geq 28.27$ kg m^{-3}) as the threshold to serve as a physical reference for the AABW. Figure R1 outlines the area covered by the AABW. It is mainly distributed from the eastern Ross Sea to the Bellingshausen Sea, from the central Weddell Sea to the Indian Ocean sector, and north of the East Antarctic continental margin from ~75°E to ~150°E.

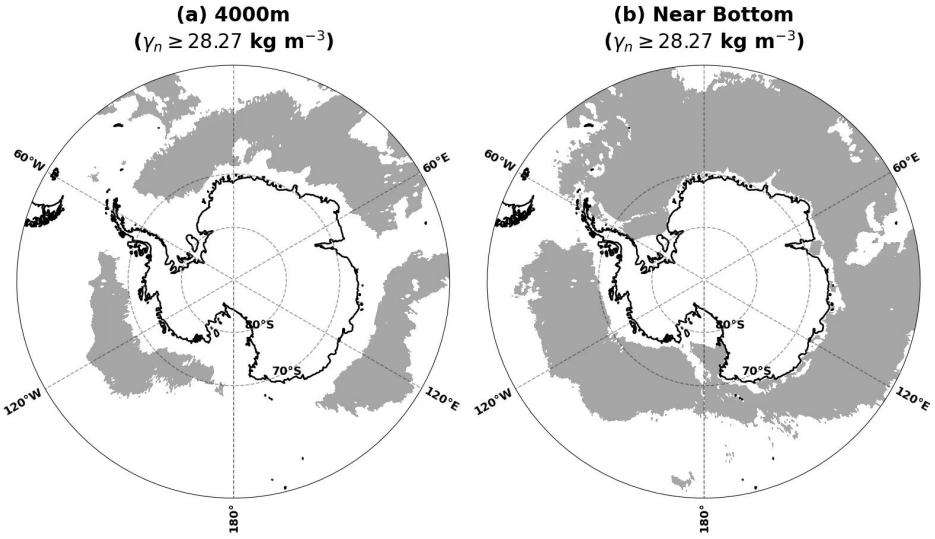

Figure R1. Spatial footprint of the Antarctic Bottom Water (AABW) defined only by the classical neutral density threshold ($\gamma_n \geq 28.27 kgm^{-3}$) across the Southern Ocean. The gray shaded regions illustrate the geographical extent of water masses satisfying this density criterion at (a) the 4000 m depth layer and (b) the near-bottom layer. The diagnostic results are derived from the World Ocean Atlas 2023 (WOA23) climatology.

Second, we know that for the cold polar waters, the thermal expansion coefficient of seawater plays a relatively minor role, making salinity the primary driver of density.

Thus we used the central salinity values of the respective water masses, including the Weddell-Prydz Bottom Water (WPBW), the Ross Sea Bottom Water (RSBW), and Adélie Land Bottom Water (ALBW), as defined by Pardo et al. (2012). Here we also conducted the sensitivity of the classification to different salinity ranges relative to these central values. In our previous manuscript, we used a salinity range of $\Delta S = \pm 0.01$ psu relative to each central salinity value, corresponding to twice the uncertainty reported by Pardo et al. (2012). Here we tested a series of thresholds, including $\Delta S = \pm 0.02, \pm 0.03, \pm 0.04$ psu. Figure R2 shows the spatial distributions of the three AABW subtypes evaluated using these progressively widened salinity thresholds at both the 4000 m and near-bottom layers. At the 4000 m depth layer, the three AABW subtypes within their respective prescribed longitudinal sectors exhibit similar spatial distribution as $\Delta S \geq 0.02$ (Figure R2). This is also true for the near bottom−layer. Table R1 provides spatial area (10^6 km^2) of each AABW subtype calculated under different salinity thresholds. It appears that the areas of the three AABW subtypes tend to slowly converge to those based on the neutral density only as $\Delta S \geq 0.02$ (Table R1). Because a salinity range wider than ±0.02 psu may incorporate diluted peripheral waters and the overlying Circumpolar Deep Water (CDW), we selected ±0.02 psu as the threshold, which provides a reasonable balance, facilitating the identification of the main bottom water bodies while mitigating the potential over-inclusion of overlying CDW. This framework reasonably delineates the bottom water distributions with distinct source-region characteristics and main advection pathways.

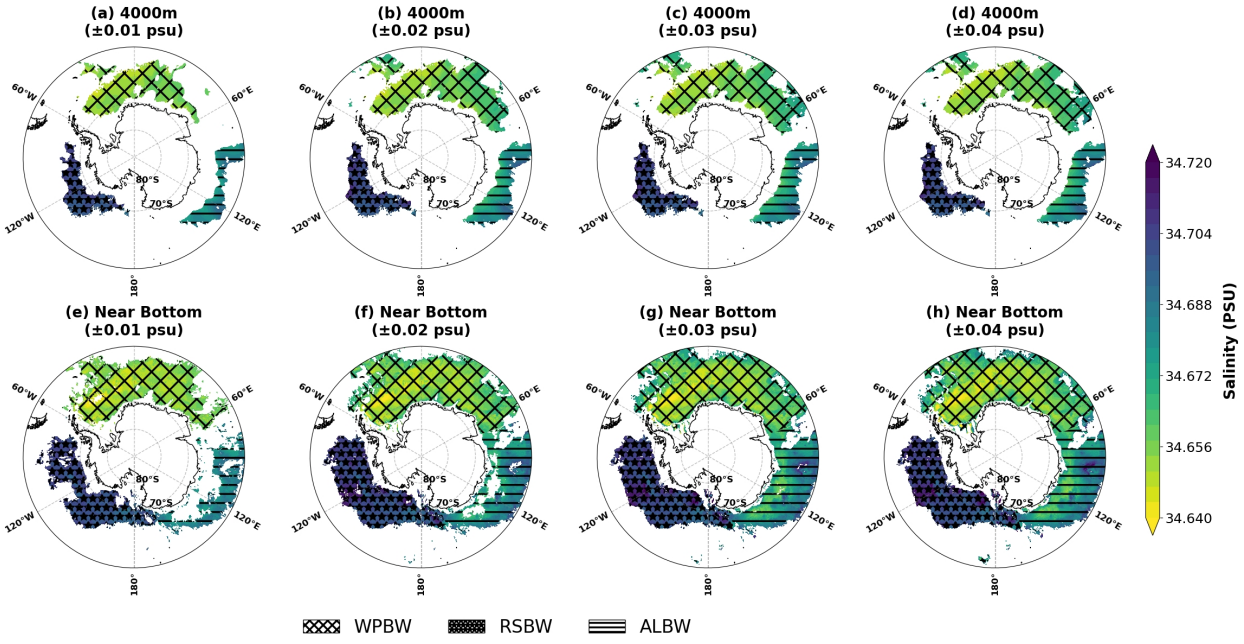

Figure R2. Spatial distributions of the identified Antarctic Bottom Water (AABW) subtypes under different salinity thresholds (ΔS). The top row (a–d) and bottom row (e–h) represent the 4000 m depth layer and the near-bottom layer, respectively. Columns from left to right show classifications based on applied ΔS values of ±0.01, ±0.02, ±0.03, and ±0.04 around the central salinity values

(WPBW: 34.650; RSBW: 34.695; ALBW: 34.683). Note that they are also constrained by the neutral density threshold ($\gamma_n \geq 28.27$ kg m^{-3}). The respective AABW subtypes are distinguished by distinct hatching patterns, as detailed in the figure legend. The background color shading represents the practical salinity field.

Table R1. Calculated areas (10^6 km^2) of the three AABW subtypes under different salinity thresholds (ΔS) at the 4000 m layer and the near-bottom layer. These thresholds are defined around the central salinity values (WPBW: 34.650; RSBW: 34.695; ALBW: 34.683).

Layer	Subtype	Neutral Density Only	±0.010	±0.020	±0.030	±0.040
4000 m	WPBW	8.36	4.96	7.56	8.30	8.36
	RSBW	2.92	2.53	2.92	2.92	2.92
	ALBW	3.25	2.03	3.10	3.25	3.25
Near-Bottom	WPBW	13.96	9.05	12.19	13.28	13.60
	RSBW	7.71	5.73	7.27	7.45	7.50
	ALBW	6.88	3.50	5.59	6.62	6.70

2. The evaluation of the reanalysis and CMIP6 models remains too qualitative.
Much of Section 3 relies on visual inspection of maps and uses fairly strong language such as models performing "relatively well", "capturing" the AABW subtypes, or "failing to capture" them. These judgments may be reasonable in a broad sense, but they are not supported by clear quantitative metrics. The paper would be much stronger if the authors added a more objective comparison... In the present version, some of the model-ranking statements feel more assertive than the evidence shown in the figures.

Response:
Thanks for the reviewer's comments. We fully agree that relying on visual comparisons of maps is insufficiently rigorous and indeed renders the descriptions of model rankings subjective. To address this issue, in the revised manuscript, we introduced quantitative evaluations to objectively and quantitatively assess all datasets.

First, we added Taylor diagrams (Figure R3) to quantitatively evaluate the fidelity of the simulated thermohaline spatial patterns across the Southern Ocean south of 50°S. Figure R3 compares the potential temperature and practical salinity fields at the 4000 m and near-bottom layers from the Ensemble Reanalysis and 16 CMIP6 models against the WOA23 climatology. In these diagrams, the spatial correlation coefficient (SCC) measures the similarity between the simulated and observed spatial patterns, while the normalized standard deviation (NSTD) indicates whether the magnitude of the simulated spatial variability is weaker or stronger than that in WOA23. The

normalized centered root-mean-square error (NCRMSE) further summarizes the combined differences in spatial pattern and variability. These metrics therefore provide a more objective basis for comparing the datasets than visual inspection of the spatial maps alone. The results show that the Ensemble Reanalysis reproduces the large-scale thermohaline structure of WOA23 with high fidelity. The SCC is calculated from spatial anomalies relative to the domain mean. The SCC for practical salinity at 4000 m reaches 0.98 (Figure R3(c)), indicating that the reanalysis closely captures the observed salinity structure of abyssal waters. In contrast, several CMIP6 models show substantial deficiencies in the spatial distribution of the deep-ocean salinity field. For example, at 4000 m, CESM2 and CIESM yield SCC values of −0.55 and −0.10, respectively. The negative correlation of CESM2 indicates that a substantial portion of its simulated salinity anomalies is spatially opposed to those in WOA23, such that regions that are relatively saline in the observations tend to be represented as relatively fresh in the model, or vice versa. The SCC of CIESM is slightly below zero, indicating little correspondence between the simulated and observed spatial salinity patterns. These discrepancies cannot be explained only by a spatially uniform saline or fresh bias. Instead, they indicate errors in the geographical placement, regional contrasts, or spatial gradients of the abyssal salinity field. Since the identification of the AABW subtypes depends partly on their characteristic salinity signatures within specific geographical sectors, such structural errors are likely to limit the models' ability to reproduce the observed spatial distributions of WPBW, RSBW, and ALBW.

Second, in the revised manuscript, we added quantitative statistical tables (Tables R2 and R3), which calculate the actual coverage areas (10^6 km^2) and mean thermohaline properties of WPBW, RSBW, and ALBW, based on the neutral density and the salinity thresholds. With these objective metrics, the performance of the reanalysis and models becomes quantitatively distinguishable. Specifically, at the 4000 m layer, WOA23 identifies WPBW, RSBW, and ALBW areas of 7.56×10^6, 2.92×10^6, and 3.10×10^6 km^2, respectively. The Ensemble Reanalysis yields corresponding areas of 7.51×10^6, 2.83×10^6, and 3.25×10^6 km^2, representing differences of approximately −0.7%, −3.1%, and +4.8% relative to WOA23. Among the CMIP6 models, CESM1-CAM5-SE-LR underestimates the spatial extent of all three subtypes, with areas of 6.39×10^6, 2.20×10^6, and 2.38×10^6 km^2, respectively. CanESM5 overestimates WPBW and RSBW, with areas of 8.26×10^6 and 3.19×10^6 km^2, but substantially underestimates ALBW at only 1.40×10^6 km^2. By contrast, several models, including CESM2, CNRM-CM6-1, and CIESM, yield zero identified areas for all three subtypes at this layer. These results reveal substantial inter-model differences not only in whether individual AABW subtype is identified, but also in the magnitude and regional distribution of their simulated spatial extents.

Based on these quantitative metrics, we have rewritten Section 3 of the original manuscript. All model-ranking and qualitative analyses are now anchored to the specific SCC, NSTD, NCRMSE, and areal statistical data.

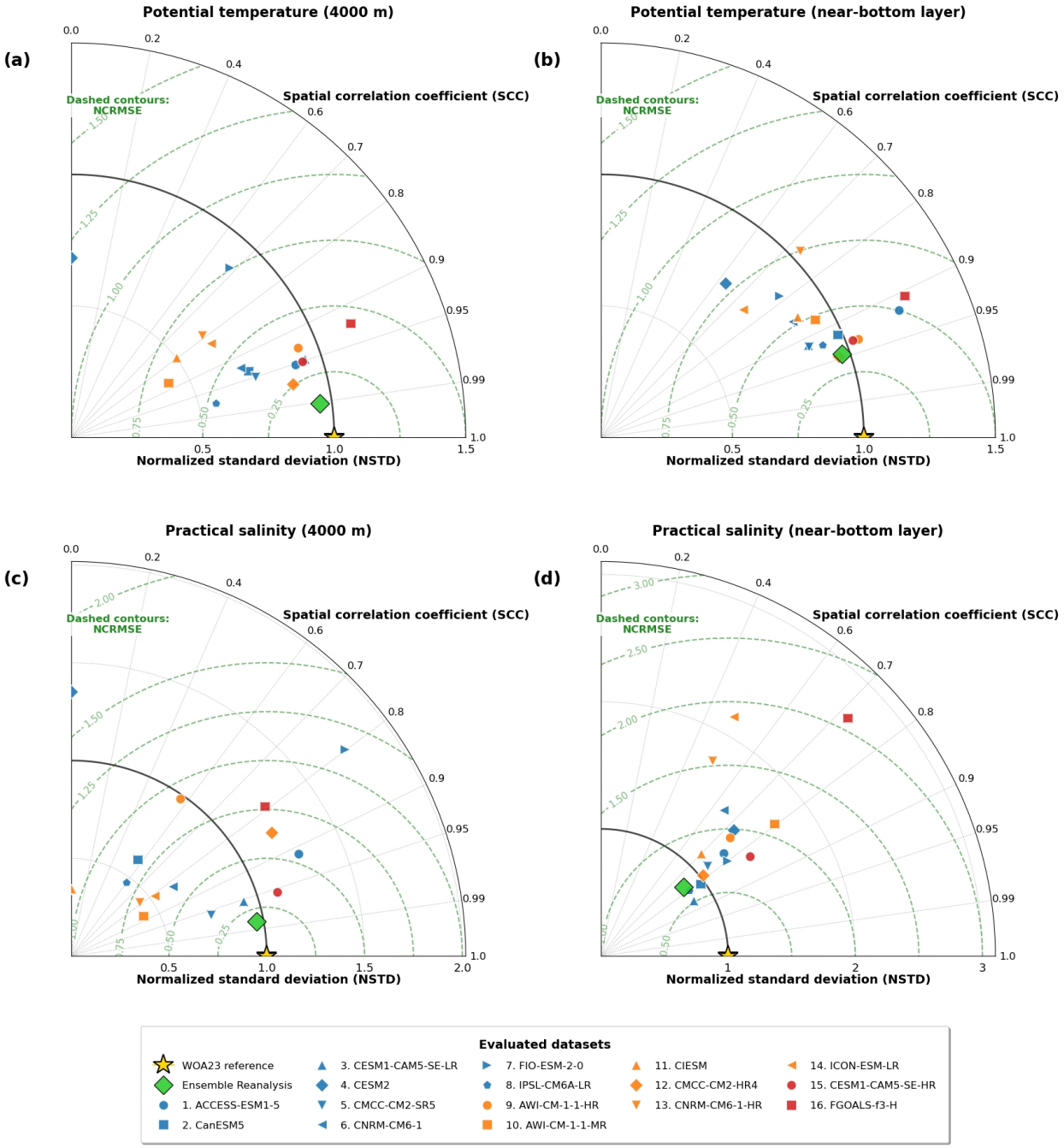

Figure R3. Taylor diagrams evaluating the ability of the simulations to reproduce the spatial distributions of thermohaline properties across the Southern Ocean south of 50°S. The upper row shows potential temperature at the 4000 m depth layer (a) and the near-bottom layer (b), while the lower row shows practical salinity at the 4000 m depth layer (c) and the near-bottom layer (d). The thermohaline spatial fields from the Ensemble Reanalysis and 16 CMIP6 models are evaluated against the WOA23 climatological reference. The gold star at SCC = 1 and NSTD = 1 represents the WOA23 reference. In each diagram, the angular coordinate represents the spatial correlation coefficient (SCC), which measures the similarity between the simulated and reference spatial distributions, while the radial coordinate represents the normalized standard deviation (NSTD), which indicates the amplitude of simulated spatial variability relative to WOA23. The green

dashed contours represent the normalized centered root-mean-square error (NCRMSE). The datasets are distinguished by color: the Ensemble Reanalysis is shown in green, low-resolution CMIP6 models in blue, moderate-resolution models in orange, and high-resolution models in red. Because the diagrams display only the non-negative-correlation quadrant, models with SCC ≤ 0 are plotted on the zero-correlation boundary. To prevent excessive stretching of the radial scale, data points with NSTD > 10 are not displayed.

Table R2. Quantitative metrics of the simulated Antarctic Bottom Water (AABW) subtypes at the 4000 m depth layer across the Southern Ocean (south of 50°S). The table details the spatial area (10^6 km²), mean potential temperature (PT, °C), and mean practical salinity (S) for the Weddell–Prydz Bottom Water (WPBW), Ross Sea Bottom Water (RSBW), and Adélie Land Bottom Water (ALBW). Metrics are evaluated for the WOA23 climatological reference, the Ensemble Reanalysis, and 16 CMIP6 models. AABW subtype properties are averaged strictly within the spatial extent where each dataset successfully satisfies the prescribed density and salinity thresholds. A value of 0 in the area column indicates that no grid cells satisfy the prescribed criteria for the corresponding subtype. In such cases, the mean potential temperature and practical salinity cannot be calculated and are therefore denoted by dashes.

Dataset	WPBW Area	WPBW Mean PT	WPBW Mean S	RSBW Area	RSBW Mean PT	RSBW Mean S	ALBW Area	ALBW Mean PT	ALBW Mean S
[Observational & Reanalysis References]									
WOA23 (Reference)	7.56	-0.55	34.657	2.92	0.04	34.701	3.10	-0.21	34.677
Ensemble Reanalysis	7.51	-0.53	34.659	2.83	0.04	34.704	3.25	-0.19	34.682
[Low-Resolution CMIP6 Models]									
ACCESS-ESM1-5	0.03	-0.29	34.631	0	-	-	0	-	-
CanESM5	8.26	-0.96	34.652	3.19	-0.49	34.689	1.40	-0.72	34.664
CESM1-CAM5-SE-LR	6.39	-0.47	34.659	2.20	0.05	34.693	2.38	-0.13	34.680
CESM2	0	-	-	0	-	-	0	-	-
CMCC-CM2-SR5	3.16	-0.20	34.667	0	-	-	0.01	0.04	34.676
CNRM-CM6-1	0	-	-	0	-	-	0	-	-
FIO-ESM-2-0	0	-	-	0	-	-	0	-	-
IPSL-CM6A-LR	8.30	-1.14	34.657	3.53	-0.85	34.683	3.42	-0.90	34.672
[Moderate-Resolution CMIP6 Models]									
AWI-CM-1-1-HR	0	-	-	2.09	-0.41	34.710	1.89	-0.80	34.695
AWI-CM-1-1-MR	0	-	-	0	-	-	0	-	-
CIESM	0	-	-	0	-	-	0	-	-
CMCC-CM2-HR4	0	-	-	0	-	-	0	-	-

CNRM-CM6-1-HR	0	-	-	0	-	-	0	-	-
ICON-ESM-LR	0	-	-	0	-	-	0	-	-
[High-Resolution CMIP6 Models]									
CESM1-CAM5-SE-HR	8.42	-0.39	34.659	1.24	0.15	34.709	0.10	-0.19	34.667
FGOALS-f3-H	4.24	-0.92	34.641	2.59	-0.02	34.689	1.59	-0.25	34.677

Table R3. Quantitative metrics of the simulated Antarctic Bottom Water (AABW) subtypes at the near-bottom layer across the Southern Ocean (south of 50°S). The variables, evaluated datasets, and spatial averaging criteria are identical to those detailed in Table R2. A value of 0 in the area column indicates that no grid cells satisfy the prescribed criteria for the corresponding subtype.

Dataset	WPBW Area	WPBW Mean PT	WPBW Mean S	RSBW Area	RSBW Mean PT	RSBW Mean S	ALBW Area	ALBW Mean PT	ALBW Mean S
[Observational & Reanalysis References]									
WOA23 (Reference)	12.19	-0.62	34.654	7.27	-0.04	34.700	5.59	-0.26	34.678
Ensemble Reanalysis	10.57	-0.56	34.658	6.33	0.04	34.704	6.01	-0.18	34.682
[Low-Resolution CMIP6 Models]									
ACCESS-ESM1-5	0.16	-0.25	34.635	0.02	-1.75	34.694	0	-	-
CanESM5	14.55	-0.87	34.653	8.09	-0.48	34.690	2.95	-0.70	34.665
CESM1-CAM5-SE-LR	10.07	-0.53	34.657	7.82	-0.02	34.691	4.81	-0.15	34.679
CESM2	0	-	-	0.05	-1.93	34.697	0	-	-
CMCC-CM2-SR5	6.75	-0.28	34.665	0.08	-0.81	34.692	0.72	0.01	34.678
CNRM-CM6-1	0	-	-	0	-	-	0	-	-
FIO-ESM-2-0	0.26	-0.26	34.669	0.03	-1.11	34.693	0	-	-
IPSL-CM6A-LR	14.95	-1.10	34.656	8.68	-0.85	34.685	6.51	-0.85	34.675
[Moderate-Resolution CMIP6 Models]									
AWI-CM-1-1-HR	0.56	-1.09	34.658	3.63	-0.44	34.708	3.13	-0.78	34.692
AWI-CM-1-1-MR	0.08	-1.24	34.650	0.08	-0.88	34.698	0.04	-0.48	34.687
CIESM	0	-	-	0	-	-	0	-	-
CMCC-CM2-HR4	0.07	-1.15	34.652	0.16	-0.54	34.695	0.05	-0.51	34.684
CNRM-CM6-1-HR	0	-	-	0	-	-	0	-	-
ICON-ESM-LR	0.01	-0.31	34.658	0.01	-0.24	34.698	0.004	-0.13	34.683
[High-Resolution CMIP6 Models]									

CESM1-CAM5-SE-HR	11.61	-0.41	34.657	3.20	0.14	34.709	0.44	-0.15	34.668
FGOALS-f3-H	5.71	-0.91	34.643	4.35	-0.07	34.689	3.89	-0.26	34.676

3. Figures 3–6 are difficult to read.

The multi-panel layout makes each individual panel very small, and it is hard to assess subtype extent or compare models systematically. This is a real problem because these figures are used to support a substantial fraction of the interpretation in Section 3. I would encourage the authors to simplify the presentation, for example, by moving the full model gallery to the Supplement and retaining only a smaller number of representative cases in the main text, ideally together with a summary figure or table that presents the main model differences more efficiently.

Response:

Thanks for the reviewer's suggestion. We agree that the original 16-panel layout was too cluttered. Following your suggestion, we restructured both the visual and quantitative presentations.

In the revised manuscript, we moved the spatial distribution maps encompassing all 16 models to the Supplementary Material for readers who are interested in looking at the performance of all models. We also generated two new figures, Figures R4 and R5, representing the native and bias-corrected states, respectively. To maximize readability, the new figures adopt an optimized 5 × 4 layout. Rather than simply selecting the "best-performing" models, we chose five representative models spanning low, moderate, and high resolutions. These five models effectively demonstrate the simulation characteristics across different resolutions discussed in the manuscript, as well as the distinctly different responses of each model to the bias correction.

CESM1-CAM5-SE-LR (low resolution): This model represents a case in which the simulated thermohaline properties fall within a reasonable range of the prescribed density and salinity thresholds of the AABW. Thus it can reasonably capture the spatial patterns of the three AABW subtypes in its uncorrected state, and the application of a regional bias correction does not further improve its performance.

IPSL-CM6A-LR (low resolution): This model represents another low-resolution case that can capture some spatial distribution features of AABW even in the absence of the specific overflow parameterization scheme discussed in the manuscript.

ACCESS-ESM1-5 (low resolution): This model represents a case strongly influenced by mean-state biases. It severely underestimates the water masses in its simulated state, but reasonably reproduces the spatial patterns of the three subtypes after applying a simple regional mean-state correction. This indicates that although the model is overall too warm/fresh, it still possesses the capability to characterize the relative spatial distribution of the water masses.

CMCC-CM2-HR4 (moderate resolution): This model represents the intermediate resolution group (25–50 km). Although most models in this group underperform, it is the only one within this resolution range capable of generating large-scale, structurally intact bottom water after bias correction.

CESM1-CAM5-SE-HR (high resolution): This model represents the high resolution group (10 km). It demonstrates that merely increasing the model resolution does not necessarily improve the AABW simulation. Furthermore, even after the mean-state correction, it still fails to generate the Ross Sea Bottom Water (RSBW), indicating that a mean-state shift cannot compensate for the fundamental lack of bottom water formation capability in certain specific regions.

Following the reviewer's suggestion, we have added new summary figures and tables with a summarized discussion in Section 3 of the main text to present the model differences efficiently and objectively. Specifically, Figures R4 and R5 visually compare the spatial distributions of the AABW subtypes across five representative models before and after bias correction, respectively, while Tables R4 and R5 quantify the spatial areas, mean potential temperatures, and mean practical salinities of the bias-corrected AABW subtypes at the 4000 m and near-bottom layers, respectively. As demonstrated by these new additions, many models struggle to capture AABW in their simulations (with CESM1-CAM5-SE-LR being an exception), while regional bias correction can enhance the performance of some models (e.g., ACCESS-ESM1-5). Furthermore, the quantitative metrics clearly show that simply increasing model resolution does not necessarily resolve simulation deficiencies.

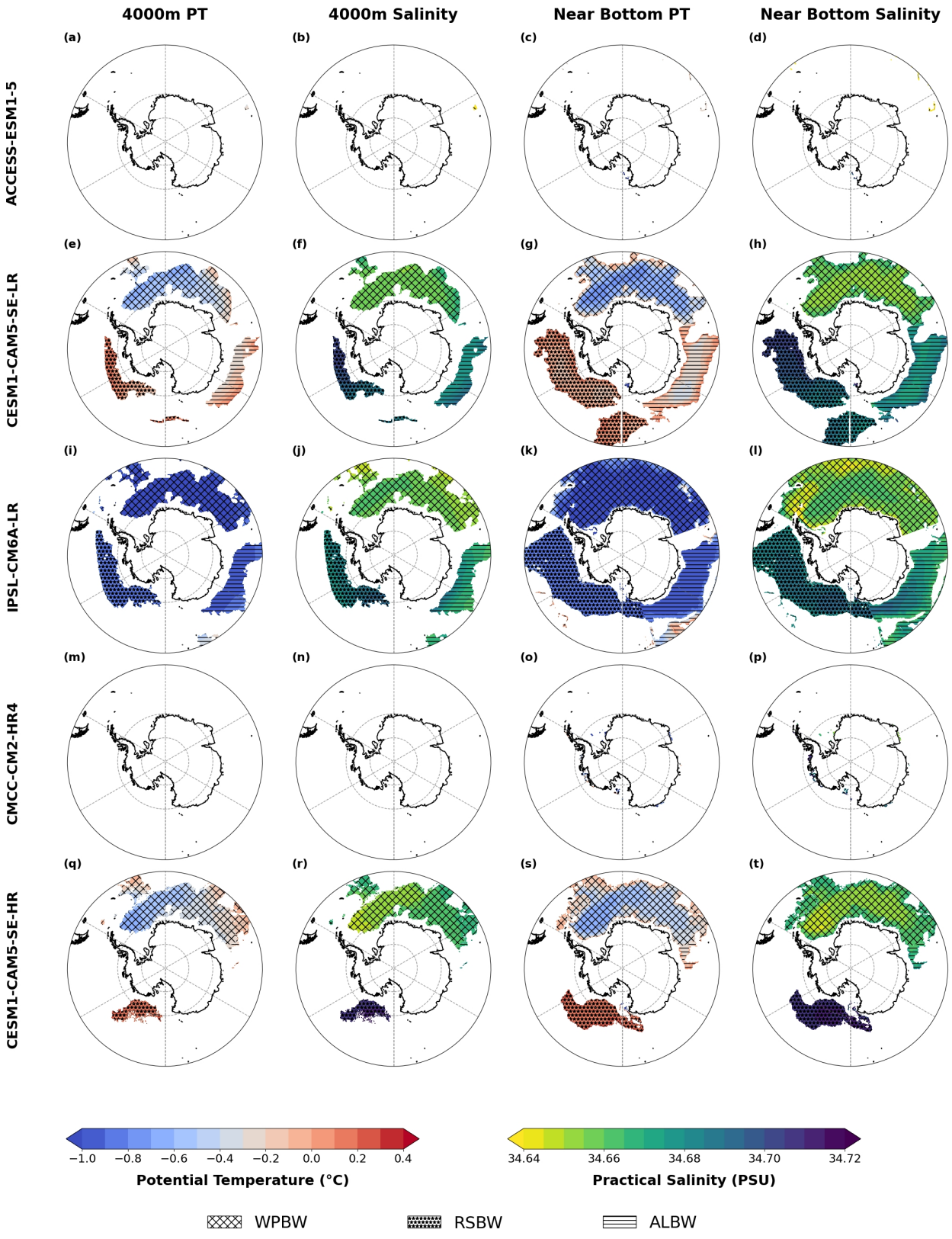

Figure R4. Spatial distributions of the native (uncorrected) simulated potential temperature and practical salinity for Antarctic Bottom Water (AABW) subtypes across five representative CMIP6

models in the Southern Ocean (south of 50°S). The figure is organized into a 5 × 4 matrix. The rows represent the strategically selected models: ACCESS-ESM1-5, CESM1-CAM5-SE-LR, IPSL-CM6A-LR, CMCC-CM2-HR4, and CESM1-CAM5-SE-HR. The columns display the evaluated thermohaline properties: potential temperature at 4000 m, practical salinity at 4000 m, potential temperature at the near-bottom layer, and practical salinity at the near-bottom layer. Subpanels are labeled from (a) to (t). The respective AABW subtypes are distinguished by distinct hatching patterns, as detailed in the figure legend.

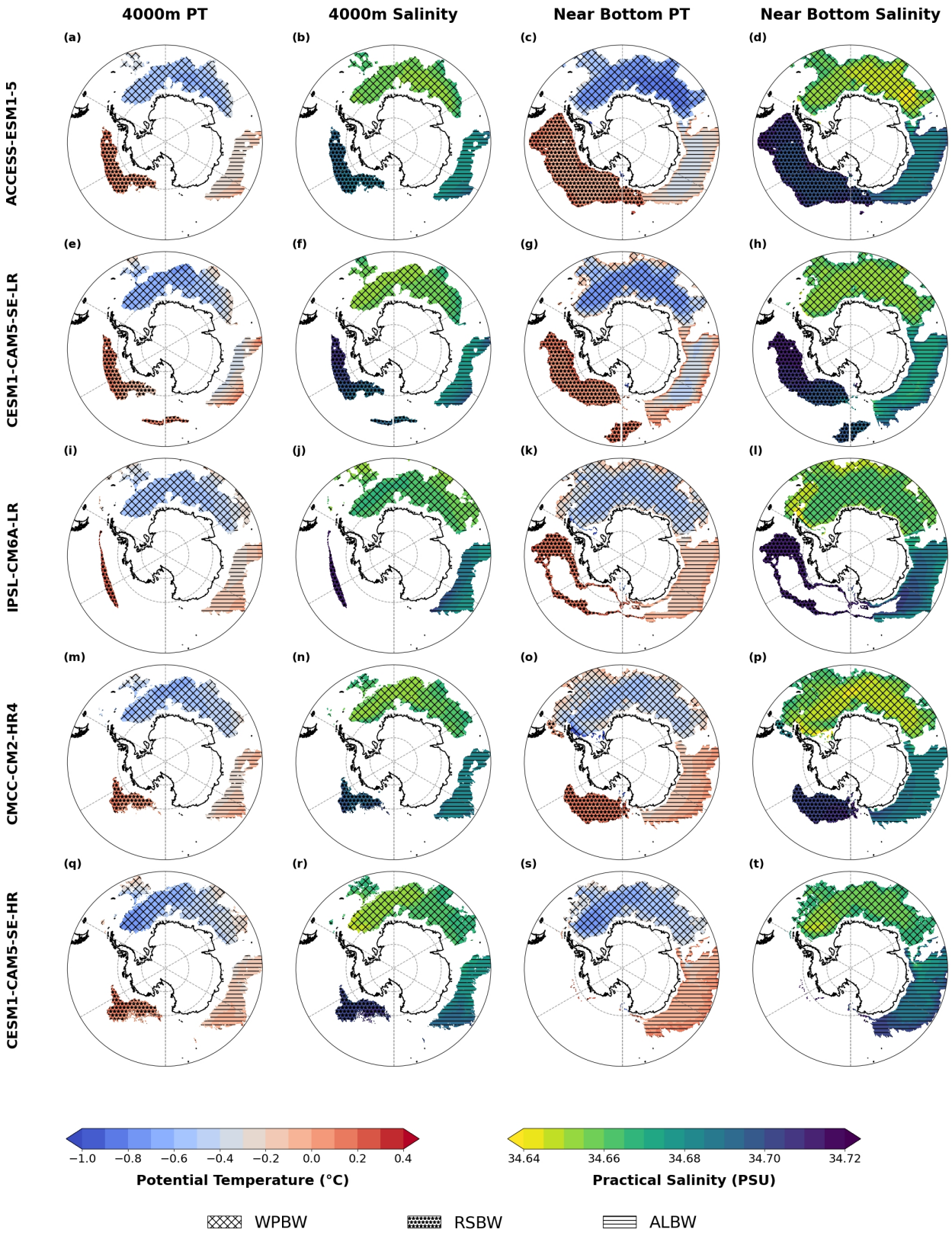

Figure R5. Spatial distributions of the bias-corrected potential temperature and practical salinity for AABW subtypes across the same five representative CMIP6 models shown in Figure R4. The

matrix layout, including the models in the rows and the thermohaline properties and depth levels in the columns, is identical to Figure R4. Subpanels are labeled from (a) to (t). The respective AABW subtypes are represented by distinct hatching patterns, as detailed in the figure legend.

Table R4. Quantitative metrics of the bias-corrected simulated Antarctic Bottom Water (AABW) subtypes at the 4000 m depth layer across the Southern Ocean (south of 50°S). The table details the spatial area (10^6 km^2), mean potential temperature (PT, °C), and mean practical salinity (S) for the Weddell–Prydz Bottom Water (WPBW), Ross Sea Bottom Water (RSBW), and Adélie Land Bottom Water (ALBW). A value of 0 in the area column indicates that no grid cells satisfy the prescribed criteria for the corresponding subtype despite the mean-state bias correction.

Dataset	WPBW Area	WPBW Mean PT	WPBW Mean S	RSBW Area	RSBW Mean PT	RSBW Mean S	ALBW Area	ALBW Mean PT	ALBW Mean S
[Low-Resolution CMIP6 Models]									
ACCESS-ESM1-5	6.20	-0.54	34.657	2.47	0.07	34.690	2.71	-0.20	34.680
CanESM5	8.17	-0.48	34.661	0.34	0.21	34.705	3.11	-0.18	34.685
CESM1-CAM5-SE-LR	6.54	-0.55	34.657	2.64	0.05	34.698	2.62	-0.21	34.680
CESM2	6.40	-0.52	34.657	1.14	0.05	34.683	1.37	-0.19	34.681
CMCC-CM2-SR5	6.38	-0.55	34.657	1.24	0.12	34.702	2.58	-0.19	34.681
CNRM-CM6-1	7.63	-0.49	34.660	2.32	0.15	34.703	3.22	-0.19	34.681
FIO-ESM-2-0	2.79	-0.61	34.646	2.15	-0.14	34.681	1.42	-0.19	34.678
IPSL-CM6A-LR	8.29	-0.47	34.661	0.64	0.21	34.714	3.21	-0.17	34.685
[Moderate-Resolution CMIP6 Models]									
AWI-CM-1-1-HR	5.93	-0.44	34.655	0.47	0.12	34.692	2.54	-0.18	34.680
AWI-CM-1-1-MR	7.41	-0.50	34.659	0.88	0.22	34.712	2.99	-0.17	34.683
CIESM	6.88	-0.53	34.659	1.37	0.12	34.699	2.74	-0.18	34.682
CMCC-CM2-HR4	7.03	-0.51	34.659	1.40	0.07	34.694	2.72	-0.17	34.684
CNRM-CM6-1-HR	7.65	-0.49	34.660	0	-	-	3.77	-0.12	34.685
ICON-ESM-LR	6.44	-0.55	34.658	1.90	0	34.695	2.60	-0.18	34.682
[High-Resolution CMIP6 Models]									
CESM1-CAM5-SE-HR	8.11	-0.51	34.659	1.80	0.08	34.703	3.42	-0.15	34.683
FGOALS-f3-H	5.89	-0.60	34.654	1.60	0	34.683	1.72	-0.18	34.680

Table R5. Quantitative metrics of the bias-corrected simulated Antarctic Bottom Water (AABW) subtypes at the near-bottom layer across the Southern Ocean (south of 50°S). The evaluated variables, bias-correction methodology, and spatial averaging criteria are identical to those detailed

in Table R4. A value of 0 in the area column indicates that no grid cells satisfy the prescribed criteria for the corresponding subtype despite the mean-state bias correction.

Dataset	WPBW Area	WPBW Mean PT	WPBW Mean S	RSBW Area	RSBW Mean PT	RSBW Mean S	ALBW Area	ALBW Mean PT	ALBW Mean S
[Low-Resolution CMIP6 Models]									
ACCESS-ESM1-5	9.71	-0.69	34.653	8.53	0	34.701	5.50	-0.26	34.686
CanESM5	12.55	-0.51	34.661	3.53	0.16	34.703	6.35	-0.17	34.692
CESM1-CAM5-SE-LR	10.58	-0.57	34.655	5.56	0.09	34.703	5.70	-0.22	34.677
CESM2	4.17	-0.43	34.666	5.17	0.01	34.691	1.70	-0.14	34.681
CMCC-CM2-SR5	11.8	-0.54	34.651	4.04	0.15	34.708	5.93	-0.14	34.675
CNRM-CM6-1	0	-	-	0.30	0.13	34.710	5.64	-0.15	34.694
FIO-ESM-2-0	2.79	-0.45	34.648	6.51	-0.10	34.692	1.77	-0.10	34.679
IPSL-CM6A-LR	13.53	-0.43	34.659	3.43	0.17	34.712	5.64	-0.13	34.688
[Moderate-Resolution CMIP6 Models]									
AWI-CM-1-1-HR	9.47	-0.61	34.650	2.52	0.07	34.697	3.90	-0.20	34.678
AWI-CM-1-1-MR	9.34	-0.54	34.665	0.07	-0.48	34.699	6.61	-0.17	34.694
CIESM	7.19	-0.64	34.668	4.95	0.17	34.709	5.29	-0.23	34.686
CMCC-CM2-HR4	12.68	-0.43	34.653	3.20	0.10	34.703	5.41	-0.09	34.685
CNRM-CM6-1-HR	0	-	-	0	-	-	0.01	0.19	34.702
ICON-ESM-LR	8.39	-0.63	34.664	5.71	0.03	34.710	6.49	-0.14	34.688
[High-Resolution CMIP6 Models]									
CESM1-CAM5-SE-HR	10.01	-0.52	34.66	0.14	-0.24	34.706	6.27	-0.03	34.689
FGOALS-f3-H	8.69	-0.88	34.654	0.03	-0.54	34.699	4.06	-0.29	34.677

Minor comments

1. Line 229: Please clarify Figure 2. The caption states that the subtype distribution is shown for 1993–1998 based on the reanalysis dataset, whereas Section 2 describes the reanalysis product as spanning 1993–2022 (e.g., Line 125). Please explain why only 1993–1998 was used here rather than the full reanalysis period. By contrast, in Figure 1, the WOA23 time period (1991–2020) appears to be consistent with the description in the data section.

Response:

We thank the reviewer for pointing this out. This was a typo in our figure caption. In fact, the subtype distribution of the reanalysis data presented in Figure 2 was calculated and plotted based on the period of 1993–2022, which is consistent with the description of the data sources in Section 2. We corrected the caption of Figure 2 to "1993–2022" in the revised manuscript.

2. Line 205: The terminology here should be WOA23 rather than WOA2023.

Response:
We thank the reviewer for pointing this out. We carefully checked the text and corrected "WOA2023" in line 205 of the revised manuscript (as well as in a few other overlooked instances in the main text) to the standard abbreviation "WOA23" to ensure the consistency of terminology throughout the manuscript.

3. The manuscript would benefit from another careful round of language editing and formatting cleanup before publication. Examples include: Line 25: "high resolution"→"high-resolution" Line 40: "under the background of"→"in the context of" Line 172: "Here"→"here" Line 211: "Consistent"→"consistent" Line 279: "reasonably"→"reasonable" Line 341: "although its spatial"→"although their spatial" Line 350: "reasonably well position"→"a reasonably good position" Line 400: "section"→"sections" Lines 436 and 438: "captures"→"capture" Line 437: "WAO23"→"WOA23"

Response:
We appreciate the reviewer's language and formatting suggestions. We corrected all the highlighted examples and conducted an additional round of proofreading throughout the revised manuscript.

Specific corrections are as follows:
Line 25 ("high resolution" → "high-resolution"): "Comparison with its high-resolution counterpart indicates that increased model resolution may not necessarily improve AABW simulations."

Line 40 ("under the background of" → "in the context of"): "Therefore, understanding the generation and variability of AABW is crucial for assessing oceanic heat budgets and biogeochemical cycles in the context of global warming."

Line 172 ("Here" → "here"): "Based on the spatial distribution of regionally sourced AABW (Solodoch et al., 2022), here WPBW is confined to the region between 60°W and 70°E..."

Line 211 ("Consistent" → "consistent"): "At the 4000 m layer, the ensemble reanalysis data indicate that, consistent with WOA23 observation, RSBW exhibits relatively high potential temperature and salinity..."

Line 279 ("reasonably" → "reasonable"): "The CESM1-CAM5-SE-LR model demonstrates a reasonable representation of the different AABW subtypes..."

Line 341 ("although its spatial" → "although their spatial"): "...all models can capture AABW subtypes to some extent, although their spatial distribution may differ from WOA23 and the reanalysis data (Figures 5–6)."

Line 350 (“reasonably well position” → “a reasonably good position”): "WPBW is captured with a reasonably good position and extent, while ALBW is confined within the longitudinal band of 75°E–135°E."

Line 400 (“section” → “sections”): "Thus, built on our analyses in sections 2 and 3, here we provide a brief analysis and comparison..."
Lines 436 and 438 (“captures” → “capture”): "The results indicate that the WOA23 data capture the distribution of WPBW, RSBW, and ALBW..." "...the ensemble reanalysis data (GLOBAL_MULTIYEAR_PHY_ENS_001_031) well capture all three AABW subtypes..."

Line 437 (“WAO23” → “WOA23”): "Compared to WOA23, the ensemble reanalysis data..."